Restricted Motion of the Lipoyl-Lysine Swinging Arm in the Pyruvate Dehydrogenase Complex of *Escherichia coli*[†,‡]

D. Dafydd Jones,[§] Katherine M. Stott, Mark J. Howard,[||] and Richard N. Perham*

Cambridge Centre for Molecular Recognition, Department of Biochemistry, University of Cambridge, 80 Tennis Court Road, Cambridge CB2 1GA, U.K.

Received December 28, 1999

ABSTRACT: The three lipoyl (E2plip) domains of the dihydrolipoyl acetyltransferase component of the pyruvate dehydrogenase (PDH) complex of *Escherichia coli* house the lipoyl-lysine side chain essential for active-site coupling and substrate channelling within the complex. The structure of the unlipoylated form of the innermost domain (E2plip^{apo}) was determined by multidimensional NMR spectroscopy and found to resemble closely that of a nonfunctional hybrid domain determined previously [Green et al. (1995) *J. Mol. Biol. 248*, 328−343]. The domain comprises two four-stranded β-sheets, with the target lysine residue residing at the tip of a type-I β-turn in one of the sheets; the N- and C-termini lie close together at the opposite end of the molecule in the other β-sheet. Measurement of ^{15}N NMR relaxation parameters and backbone hydrogen/deuterium (H/D) exchange rates reveals that the residues in and surrounding the lipoyl-lysine β-turn in the E2plip^{apo} form of the domain become less flexible after lipoylation of the lysine residue. This implies that the lipoyl-lysine side chain may not sample the full range of conformational space once thought. Moreover, reductive acetylation of the lipoylated domain (E2plip^{holo} → E2plip^{redac}) was accompanied by large changes in chemical shift between the two forms, and multiple resonances were observed for several residues. This implies a change in conformation and the existence of multiple conformations of the domain on reductive acetylation, which may be important in stabilizing this catalytic intermediate.

The pyruvate dehydrogenase (PDH)[1] complex catalyzes the oxidative decarboxylation of pyruvate, transferring the resultant acetyl group to coenzyme A. It belongs to a family of related 2-oxo acid dehydrogenase complexes, which includes the 2-oxoglutarate (2OGDH) and branched-chain 2-oxo acid (BCDH) dehydrogenase complexes. In the PDH complex, the three component enzymes are pyruvate decarboxylase (E1p; EC 1.2.4.1), dihydrolipoyl acetyltransferase (E2p; EC 2.3.1.12) and dihydrolipoyl dehydrogenase (E3; 1.8.1.4) (reviewed in refs *1*−*3*). The 2-oxo acid decarboxylase (E1p, E1o, or E1b) catalyzes the initial decarboxylation of the 2-oxo acid, using thiamin diphosphate (ThDP) as a cofactor, and the subsequent reductive acylation of the dithiolane ring of the lipoyl group attached to a lysine residue in the lipoyl domain(s) of the E2 component. The dihydrolipoyl acyltransferase (E2p, E2o, or E2b) is responsible for the transfer of the acyl group to CoA. The reoxidation of the dihydrolipoyl group to reform the dithiolane ring, with NAD^+ as the ultimate electron acceptor, is catalyzed by E3.

In the PDH complex from *Escherichia coli*, E2p forms a cubic core consisting of 24 polypeptide chains arranged with octahedral symmetry; E1 and E3 are bound tightly but noncovalently to the core, with E1 probably associated preferentially with the 12 edges of the cube and E3 with the six faces (*1*, *3*, *4*). The independently folded lipoyl domain(s) forms the N-terminal part of the E2 chain. The number of lipoyl domains per E2p chain can vary, e.g., from one in *Bacillus stearothermophilus* and yeast to three in *E. coli*. Acting as a "swinging arm" (*5*), the lipoyl group visits each of the three active sites (E1p, E2p, and E3) of the complex and provides the basis of active-site coupling.

The lipoyl domain also plays a vital role in coupling the reactions within the complex in an organized and specific manner (*1*−*4*). Free lipoate can act as a substrate for E2p and E3 but is a very poor substrate for E1p, in contrast with the lipoylated domain (for which k_{cat}/K_m is raised by a factor of 10^4) (*6*). Moreover, the E2o and E2p lipoyl domains from *E. coli* (*6*, *7*) and *Azotobacter vinelandii* (*8*) can function as substrates only with their cognate E1o or E1p. Thus, the lipoyl domain provides a mechanism for substrate "activation" and channelling, such that reductive acylation is confined to a lipoyl group covalently attached to a specific lysine residue of the intended E2 component (*1*). In the E2

[†] We thank the Biotechnology and Biological Sciences Research Council for the award of a research grant (to R.N.P.) and the BBSRC and The Wellcome Trust for support of the core facilities of the Cambridge Centre for Molecular Recognition. D.D.J is grateful to the BBSRC and AdProTech for the award of a CASE Studentship.

[‡] The coordinates of the 30 structures comprising the ensemble have been deposited in the Protein Data Bank under the accession number 1qjo.

* To whom correspondence should be addressed. Phone: +44 1223 333663. Fax: +44 1223 333667. E-mail: r.n.perham@bioc.cam.ac.uk.

[§] Present address: MRC Centre for Protein Engineering, Hills Road, Cambridge CB2 2QH, U.K.

[||] Present address: MRC Unit for Protein Function and Design, University Chemical Laboratory, Lensfield Road, Cambridge CB2 1EW, U.K.

[1] Abbreviations: E2p, dihydrolipoyl acetyltransferase; E2plip, innermost lipoyl domain of *E. coli* E2p; E2plip^{apo}, unlipoylated E2plip domain; E2plip^{holo}, lipoylated E2plip domain; E2plip^{redac}, reductively acetylated domain; H/D, hydrogen/deuterium; hetNOE; heteronuclear NOE; HSQC, heteronuclear single quantum correlation; LplA, lipoyl protein ligase A; NMR, nuclear magnetic resonance; NOE, nuclear Overhauser effect; PDH, pyruvate dehydrogenase; T_1, spin−lattice relaxation time; T_2, spin−spin relaxation time.

10.1021/bi992978i CCC: $19.00
Published on Web 06/30/2000

chain, the lipoyl domain is followed by a small (4 kDa) peripheral subunit-binding domain (*9*-*11*) and, at the C-terminus, by the much larger (28 kDa) dihydrolipoyl acyltransferase domain, which is also responsible for aggregating to form the cubic core (*12*, *13*). These domains are separated by long (25−30 residue) flexible but extended linker regions that facilitate movement, especially of the lipoyl domains, as part of the system of coupling physically dispersed active sites (*1*-*4*).

Solution structures of a hybrid (outermost with innermost) E2p lipoyl domain (*14*) and E2o lipoyl domain (*15*) derived from *E. coli* PDH and 2OGDH complexes, respectively, have been solved by multidimensional NMR spectroscopy, along with others from different organisms (*16*−*19*). Their overall backbone structures are virtually identical, in each instance consisting of a flattened β-barrel comprising two four-stranded β-sheets with a 2-fold axis of quasi-symmetry. The lipoyl-lysine residue is located at the tip a protruding type I β-turn in one sheet and the N- and C-termini are close together in space in the other β-sheet. Positioning the target lysine in the β-turn is critical for correct posttranslational modification by the lipoylation machinery of the *E. coli* cell (*20*); the prominent surface loop linking β-strands 1 and 2, which lies close in space to the lipoyl-lysine β-turn, is important for the structure and function of the domain, notably its interaction with the E1 component (7, *21*). The structure of the related lipoyl-containing component of the pea leaf glycine cleavage system, designated the H-protein, has been determined by X-ray crystallography (*22*−*24*) and NMR spectroscopy (*25*), and similar considerations are likely to apply.

The structure of the 2-oxo acid dehydrogenase lipoyl domain is not substantially affected by posttranslational modification, and the lipoyl-lysine side chain is essentially free to rotate, as judged by spin labeling of the lipoyl group (*26*, *27*) and NMR studies of chemical shift changes between the apo- and holo-domains (*28*, *29*). In contrast, the lipoyl group of the uncharged H-protein appears to be relatively fixed in orientation and, after it has been reductively aminomethylated by the glycine decarboxylase component, retreats into a nearby cleft on the protein surface, where it becomes essentially immobilized (*23*, *25*). The hydrophobic environment protects the labile reaction intermediate (*23*), making it a perfect example of the "hot potato" hypothesis" of multienzyme complex action (*1*). It has been suggested that the 2-oxo acid dehydrogenase lipoyl domains may play a comparable role in helping to stabilize the thioester linkage in the reductively acylated lipoyl group (*7*).

The structure of a native, functional lipoyl domain of *E. coli* E2p has not hitherto been determined. The hybrid domain constructed from the outermost and innermost lipoyl domains used previously contained a glutamine residue in place of the lipoyl-lysine (*14*). Here we describe the solution structure of the innermost lipoyl domain of *E. coli* E2p determined by means of NMR spectroscopy. We go on to investigate the effect of lipoylation and reductive acetylation on the structure of the domain by monitoring the changes in chemical shift, ^{15}N relaxation times, ^{1}H-^{15}N heteronuclear NOE enhancements and hydrogen/deuterium (H/D) exchange rates that accompany these processes. The results throw new light on the part played by the lipoyl domain and its function as a catalytic intermediate.

MATERIALS AND METHODS

Preparation of the Apo-, Holo-, and Reductively Acetylated Forms of the Innermost E2p Lipoyl Domain. The unlipoylated and uniformly ^{15}N-labeled form of the innermost lipoyl domain of *E. coli* E2p (E2plip^{apo}) was prepared by expressing a sub-gene present in a pET11c vector (E. L. Roberts and R.N.P., unpublished work) in *E. coli* BL21 DE3 cells in a modified version of the morpholinepropanesulfonate (Mops) minimal medium (*30*). The minimal medium contained 10 mM $^{15}NH_4Cl$ as the sole nitrogen source. Unlabeled E2plip was obtained similarly, except that the cells were grown in 2TY medium. The domain was purified in the unlipoylated form as described previously (7, *15*, *31*).

The purified apo-domain was lipoylated in vitro using the recombinant lipoate protein ligase, LplA, based on a procedure described previously (*7*, *32*). The reaction mixture contained 20 mM Tris-HCl, pH 7.5, 5 mM $MgCl_2$, 5 mM ATP, 2.5 mM R-lipoic acid (Asta Pharmaceuticals), 1 mM E2plip^{apo}, and 200 μg/mL LplA. The reaction mixture was left in the dark at room temperature until the domain was fully lipoylated, as judged by electrospray mass spectrometry. The products were separated by anion-exchange chromatography using a Resource-Q column (Pharmacia) developed with an ammonium bicarbonate gradient. The lipoylated domains were buffer-exchanged into 20 mM sodium phosphate, pH 6.85.

Reductive acetylation of the domain was carried out as described previously (*7*, *33*). To 0.6 mM ^{15}N-labeled lipoylated E2p lipoyl domain (E2plip^{holo}) in 20 mM sodium phosphate, pH 6.85, were added 0.1 mM ThDP−Mg, 0.1 μM E1p and 2 mM pyruvate. After 1 h at 25 °C, the domain was fully reductively acetylated, as judged by electrospray mass spectrometry. Two samples were prepared in this manner. The first was exchanged into fresh 20 mM sodium phosphate buffer, pH 6.85, whereas the second was left in the original reaction buffer. Both samples produced very similar heteronuclear single quantum correlation (HSQC) NMR spectra when examined subsequently.

NMR Spectroscopy. For NMR spectroscopy, protein samples at a concentration of 0.6 mM were made up in 20 mM sodium phosphate (at pH 6.85 for backbone dynamics and pH 5.5 for initial resonance assignments) in 90% $^{1}H_2O$/10% $^{2}H_2O$. Spectra were recorded on either a Bruker AM500 or DRX500 spectrometer. All data were processed using the AZARA software package (W. Boucher, unpublished work) and analyzed with the program ANSIG 3.3 (*34*). The two-dimensional (2D) DQF-COSY (*35*), TOCSY (*36*), NOESY (*37*), HMQC-TOCSY, and HMQC-NOESY (*38*) spectra were recorded at 298 and 307 K and used to assign the resonances of the E2plip^{apo} domain.

Backbone Dynamics of the E2plip^{apo} and E2plip^{holo} Domains. The ^{1}H-^{15}N heteronuclear nuclear Overhauser effect (hetNOE) enhancements of the E2plip^{apo} and E2plip^{holo} domains were determined from heteronuclear (^{15}N-^{1}H) correlation experiments performed with and without preceding proton saturation (*39*, *40*). A control experiment without proton saturation was also performed in order to calculate the error. The heteronuclear steady-state NOE enhancements were derived from peak intensities according to the definition of Schirmer et al. (*41*).

^{15}N spin−lattice (T_1) relaxation times were obtained using a modified HSQC experiment (*39*, *42*, *43*). ^{15}N T_1 data were obtained using delays of 20, 1000, 60, 680, 160, 480, 260, and 20 ms, recorded in that order. The 20 ms delay experiment was repeated in order to calculate the error. ^{15}N spin−spin (T_2) relaxation times were obtained using inverse detection (HSQC) experiments (*40*) which incorporated a ^{15}N spin−echo sequence for the determination of T_2. ^{15}N T_2 relaxation times were obtained using delay values of 7.92, 300.96, 47.52, 142.56, 79.2, 205.92, 15.84, and 7.92 ms, recorded in that order; the 7.92 ms delay experiment was repeated in order to calculate the error. T_1 and T_2 relaxation rate constants for individual residues were obtained from a fit of intensity to the classical equation $I_i = I_0 \exp -(t/T_x)$, where I_i is the intensity of the relevant signal at time i, I_0 is the intensity at time 0, t is the time delay and T_x is the relaxation time.

The H/D exchange rates of the amide protons for E2plip^{apo} and E2plip^{holo} were determined by recording a series of HSQC spectra of lyophilized protein samples immediately after they had been redissolved in ^2H_2O.

Structural Constraints and Structure Calculations for the E2plip^{apo} Domain. Through-space NOE connectivities were obtained from 2D NOESY experiments (*37*) at 298 and 307K. Cross-peaks that exhibited strong, medium, weak, and very weak intensities were converted into distance restraints of <2.5, <3.5, <5.0, and <6.0 Å, respectively. Vicinal coupling constants between the $^1H^N$ and $^1H^\alpha$ spins ($^3J_{\alpha N}$) were estimated using a DQF-COSY experiment. The distance between the two peaks in each cross-section yields the approximate $^3J_{\alpha N}$ coupling constants. Estimates of the backbone ϕ were made by reference to a Karplus curve (*44*). Using a combination of the NOESY, a short mixing time TOCSY and a 2D version of the HNHB experiment (*45*), the most populated χ_1 rotamer was determined for 12 valine residues and 18 β-methylene protons. Slowly exchanging amides were identified as described above. A total of 39 hydrogen bond donors were included in the final restraint list.

Structures were calculated from the NMR data using the program X-PLOR (*46*), but with minor modifications to the files random.inp, sa.inp, and refine.inp from X-PLOR 3.1 release (M. Nilges, personal communication). The computations were performed starting from random initial structures and using "sum" averaging with an r^{-6} potential (*47*) for all atoms.

General Methods. Protein purification was carried out on a Pharmacia FPLC at 4 °C and column fractions were analyzed by SDS−PAGE using the Pharmacia Phastsystem. Electrospray mass spectrometry of the various forms of E2plip was performed as described previously (*7*). All protein concentrations were determined by amino acid analysis, kindly performed by Mr. Peter Skerritt of the PNAC Facility, Department of Biochemistry, University of Cambridge. LplA was purified as described elsewhere (*32*) and E1p was purified from *E. coli* cells overexpressing the sub-gene for E1p present in the pET11d plasmid (P. A. Reche, unpublished work).

RESULTS

Preparation of the E2plip^{apo} Domain and Its Lipoylated (E2plip^{holo}) and Reductively Acetylated (E2plip^{redac}) Forms. Residues Val2−Ala80 of the innermost E2p lipoyl domain correspond to residues Val205−Ala283 in the intact E2p polypeptide chain. Owing to the nature of the expression system, the E2plip domain was purified in its apo-form (E2plip^{apo}), as described previously (*7*), in both unlabeled and ^{15}N-labeled versions. The identity of the domain and the extent of incorporation of the ^{15}N isotope (97%) were established by electrospray mass spectrometry (Table 1). Partial processing of the N-terminal methionine residue was noted, as observed previously (*7*). The apo-domain was posttranslationally modified in vitro using the recombinant *E. coli* LplA in the presence of R-lipoic acid and ATP−Mg, as described in the Materials and Methods. Mass spectrometry (Table 1) showed the mass of the ^{15}N-labeled domain to have increased in size by 188 Da, corresponding to the addition of a single lipoyl group. Reductive acetylation of the lipoylated domain (E2plip^{holo}) was achieved by addition of a catalytic amount of E1p and pyruvate, as described in the Materials and Methods. Mass spectrometry (Table 1) showed the only major protein species present to have a mass 44 Da higher than that of the lipoylated domain, corresponding to full reductive acetylation.

Table 1: Electrospray Mass Spectrometry of the Various Forms of the ^{15}N-Labeled E2plip Domain[a]

species	theoretical mass (Da)		measured mass (Da)	
	−Nmet	+Nmet	−Nmet	+Nmet
E2plip^{apo}	9206	9339	9203 ± 0.7	9335 ± 1.0
E2plip^{holo}	9394	9527	9392 ± 0.5	9524 ± 0.2
E2plip^{redac}	9438	9571	9436 ± 0.3	9568 ± 0.9
E2plip^{redac} (after NMR)			9394 ± 0.9	9525 ± 1.6
			9436 ± 1.2*	9569 ± 2.3*

[a] The domains were prepared and analyzed as described in the Materials and Methods. (*) The major peak in a spectrum. The theoretical masses were calculated using the program PAWS (Proteometrics).

After the E2plip^{redac} domain had been used for NMR spectroscopy, it was examined again by mass spectrometry. A new species that represented ca. 30% of the total protein was detected, the molecular mass of which suggests it was the reduced but deacetylated E2plip domain (Table 1). The lability of the thioester linkage in the reductively acetylated lipoyl group has been noted previously, most obviously in the reductively succinylated lipoyl domain of *E. coli* E2o (*7*, *8*, *48*). The present evidence demonstrates that the *E. coli* E2p domain can be fully reductively acetylated but indicates that the thioester linkage is slowly hydrolyzed under the applied conditions.

NMR Assignment Strategy. Initially, peaks were assigned to the E2plip^{apo} domain according to amino acid type from DQF-COSY, TOCSY, HSQC, and HMQC-TOCSY experiments at 298 and 307K. Sequential assignments were established using through-space connectivities derived from NOESY and HMQC-NOESY spectra at 298 and 307K. The HSQC spectra of the E2plip^{holo} and E2plip^{redac} domains were assigned by comparison with the spectra of the E2plip^{apo} domain. Assignment of significantly shifted peaks was confirmed using HMQC-NOESY experiments.

Structure Calculations for the E2plip^{apo} Domain. An ensemble of structures of the E2plip^{apo} domain was computed from simulated annealing calculations using 799 intraresidue and 777 interresidue unambiguous distance restraints, 31 ϕ

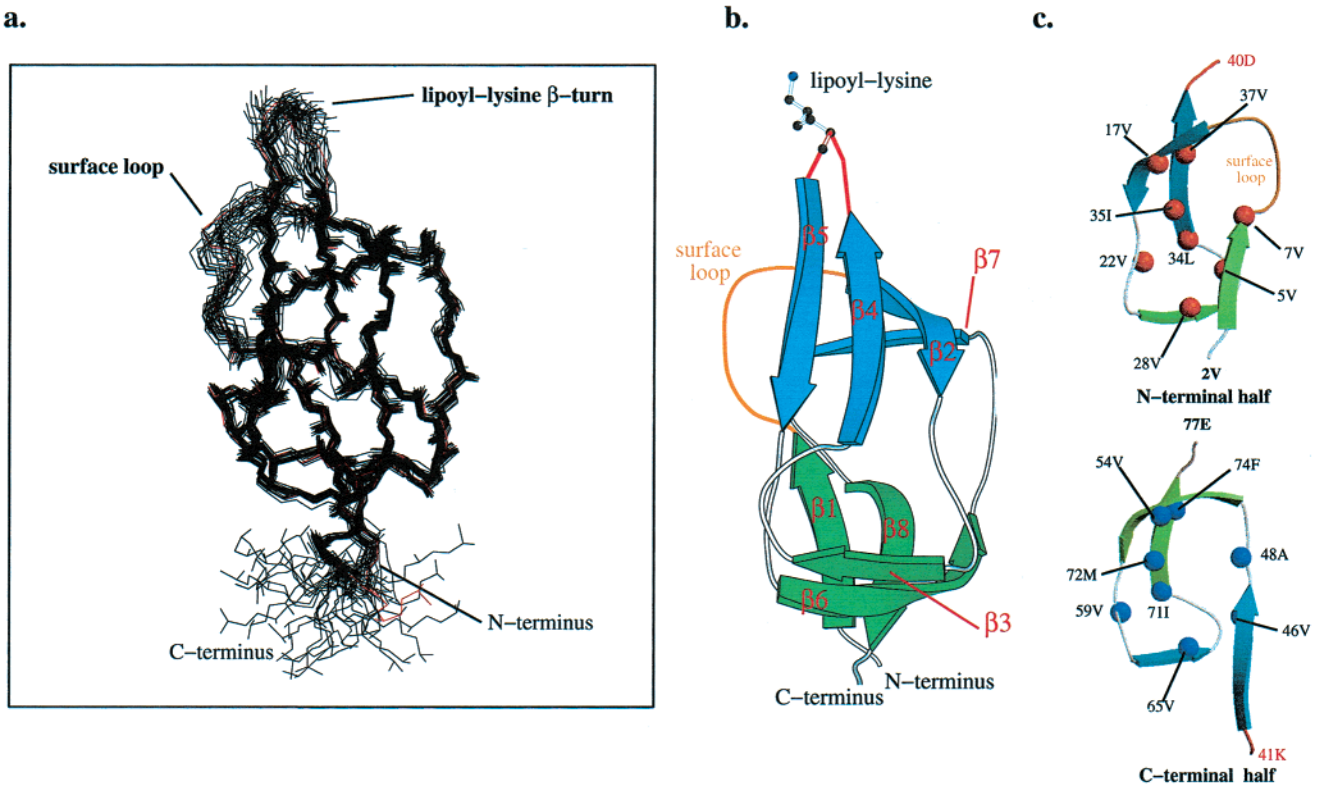

FIGURE 1: Structure of the *E. coli* E2plip^{apo} domain. (a) The backbone trace of an ensemble of 30 structures. (b) Schematic representation of the E2plip^{apo} domain. The two β-sheets are shown as blue and green, with the four strands in each sheet labeled sequentially from the N-terminus. The prominent surface loop linking β-strands 1 and 2 is indicated in orange and the lipoyl-lysine β-turn in red. (c) Comparison of the N- and C-terminal halves of the domain and the positioning of key hydrophobic core residues. All diagrams were prepared using the program MOLSCRIPT (*58*).

and 30 χ_1 dihedral angle restraints, and 39 hydrogen bond assignments. The backbone trace shown in Figure 1 contains 30 structures (those with the lowest energy and no distance violations > 0.5 Å) out of a total of 60 structures.

The structure is well-defined apart from the C-terminal segment (residues 78 onward), which forms part of the flexible region that links the lipoyl domain with the other E2p domains (*1*). Over residues 2−77, the root-mean-square deviation (rmsd) is 0.633 Å for the backbone and 1.124 Å for all heavy atoms for the ensemble of structures. Two regions show a higher rmsd than the majority of the backbone: the prominent surface loop (residues 9−14) linking β-strands 1 and 2 and the type I β-turn (residues 39−42) housing the lysine residue that is the target for lipoylation. If these two regions are omitted, the rmsds for the backbone and all heavy atoms fall to 0.500 and 0.983 Å, respectively. The structures have good covalent geometry, as judged by PROCHECK (*49*); for a list of relevant statistics, see Table 2.

Structure of the E2plip^{apo} Domain. The structure of this native lipoyl domain of *E. coli* E2p is very similar to that determined for a hybrid domain (*14*), with a backbone rmsd between the two structures of 1.25 Å. It has the fold of a flattened β-barrel, composed of two β-sheets with a 2-fold axis of quasi-symmetry, characteristic of other lipoyl domains of 2-oxo acid dehydrogenase complexes (*14*−*19*). One β-sheet is composed of strands 1, 3, 6, and 8 and the other of strands 2, 4, 5, and 7 (Figure 1b). The N- and C-termini lie close in space at one end of the protein, with the type I β-turn housing the lipoyl-lysine residue at the other end of the molecule in the second β-sheet (Figure 1b). Apart from the quasi-symmetry relating the β-sheets, there is also quasi-symmetry relating to the N- and C-terminal halves of the domain and what constitute the hydrophobic core residues (Figure 1c).

Table 2: Structural Statistics for the Final Ensemble of 30 Structures for the E2plip^{apo} Domain[a]

	$\langle SA\rangle_{ens}$	$\langle SA\rangle_{clo}$
rmsd deviation from the mean structure for the final ensemble of structures		
backbone (Å)		
residues 2−77	0.633	0.516
residues 2−10; 15−39; 43−77	0.500	0.382
all heavy atoms (Å)		
residues 2−77	1.124	1.021
residues 2−10; 15−39; 43−77	0.983	0.811
rmsd from restraints and idealized geometry		
NOE distances (Å)	0.038 ± 0.0009	0.038
dihedral angles (deg)	0.24 ± 0.29	0.307
bonds (Å)	0.0022 ± 0.000 06	0.0022
angles (deg)	0.319 ± 0.005	0.304
impropers	0.12 ± 0.0033	0.129
E_{NOE} (kcal/mol)	56.5 ± 2.7	56.7
E_{L-J} (kcal/mol) before minimization	−71.7 ± 14	−77.5
E_{L-J} (kcal/mol) after minimization	−266.4 ± 9.6	−277.6
assessment of backbone quality according to the Ramachandran plot		
most favored region (%)	55.9	63.6
additionally allowed region (%)	39.9	31.8

[a] $\langle SA\rangle_{ens}$ refers to the statistics for the ensemble and $\langle SA\rangle_{clo}$ refers to the statistics for the structure closest to the mean coordinates. The rmsd values were calculated using the UWMN program (Hartshorn et al., 1990−1991, unpublished work). The rmsds from the restraints and geometry were generated by X-PLOR (*46*). The assessment of backbone quality according to the ramachandran plot was calculated using PROCHECK−NMR (*49*).

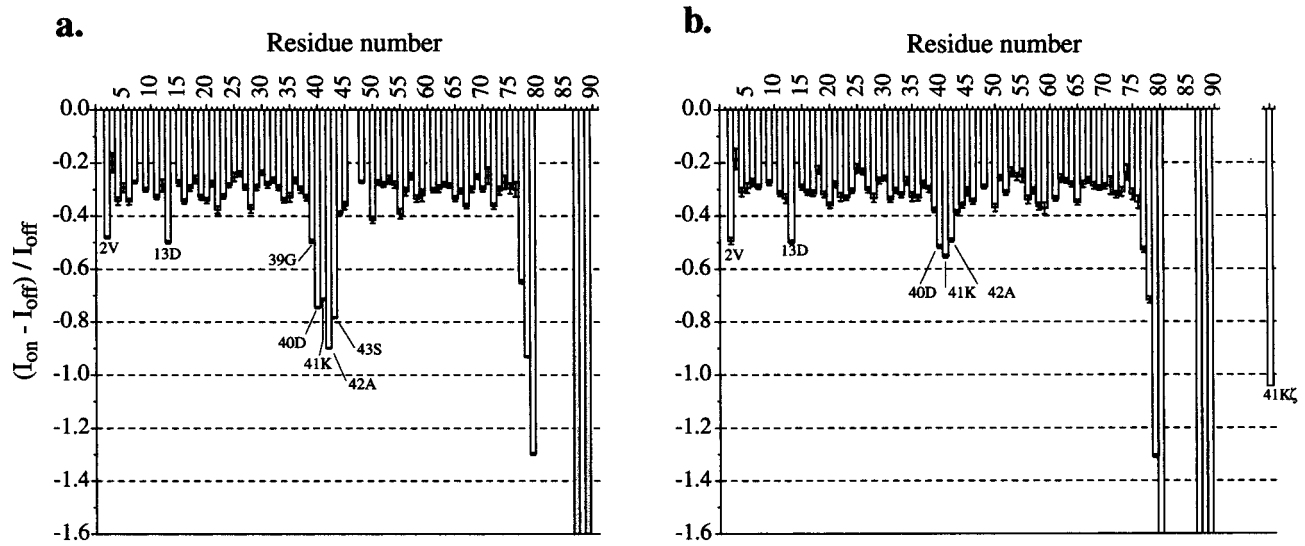

FIGURE 2: ^{1}H-^{15}N heteronuclear NOE values of the (a) E2plip^{apo} and (b) E2plip^{holo} domains. I_{on} represents the intensity of the cross-peak with the application of the proton saturation giving rise to NOE enhancements and I_{off} represents the intensity in the absence of the NOE.

As noted previously, the structures of the biotinylated domains of *E. coli* acetyl-CoA carboxylase (*50*-*53*) and *Propionibacterium shermanii* transcarboxylase (*54*) are closely similar.

The hydrophobic core residues are generally conserved in lipoyl domains and biotinyl domains, consistent with their being critical in the generation of the common fold. Other conserved residues include several proline and glycine residues responsible for the turns in the structure. Apart from the type-I β-turn housing the lipoyl-lysine, there are also four type-II β-turns that give rise to the "hammer-head" motif (Figure 1c) present in each half of the structure (*51*); each motif contains a conserved glycine residue that initiates a type-II β-turn. Another feature common to lipoyl domains is the presence of an exposed surface loop linking β-strands 1 and 2, which is present only in one-half of the domain (Figure 1, panels b and c). As in the structures of all other lipoyl domains determined thus far, this surface loop is relatively poorly defined (Figure 1a) owing to a lack of long-range NOEs from the surface loop to the rest of the protein or to its innate flexibility.

Backbone Dynamics of the E2plip^{apo} Domain. Analysis of the ensemble of structures for the E2plip^{apo} domain identified three regions with an rmsd significantly higher than that of the majority of the backbone average: the surface loop linking β-strands 1 and 2 (residues 9−14), the lipoyl-lysine β-turn (residues 39−42) and the C-terminal tail (residue 78 onward). Three major NMR parameters were investigated on a residue-by-residue basis: the ^{1}H-^{15}N heteronuclear steady-state NOE enhancements and the ^{15}N spin−lattice (T_1) and ^{15}N spin−spin (T_2) relaxation times. Each of these parameters is sensitive to internal motions on different time scales. Heteronuclear NOE and ^{15}N T_1 relaxation times are sensitive to high frequency (rapid internal) motion on the picosecond to nanosecond (10^9−10^{12} s^{-1}) time scale, whereas the ^{15}N T_2 relaxation time is sensitive to motions on a millisecond time scale. In addition, T_1 and T_2 are sensitive to the overall tumbling of the molecule.

The residues in the C-terminal tail show the lowest (most negative) hetNOE values, confirming the flexibility of this region (Figure 2a). The hetNOE values in the lipoyl-lysine β-turn, more specifically residues Gly39−Ser43, also show a significant difference from those of the majority of the polypeptide backbone, suggesting that this β-turn is flexible. The only residue in the surface loop linking β-strands 1 and 2 with a hetNOE more negative than that of the majority of the backbone is Asp13. Likewise, the hetNOE value for Val2 was also significantly more negative than the average for the rest of the backbone, implying that this residue is more mobile. This could be due to its being the residue where the innermost lipoyl domain is joined to the linker region that tethers it to the outer two lipoyl domains.

Analysis of the T_1 relaxation times indicates that residues Val2, Asp9, Gly12, Glu14, Asp40, Lys41 (the target for lipoylation), Ser43, and Val59 exhibited T_1 relaxation times slightly above the backbone T_1 values (Figure 3a). In addition, Ala42 (Figure 3a) and the C-terminal tail region (results not shown) have T_1 relaxation times far higher than the majority of the backbone amide nitrogens. The T_1 values correlate well with the ^{15}N T_2 relaxation times: residues Val2, Asp13, Val14, Val22, Asp40, Lys41, and Val59 all had T_2 values above the majority of the backbone values, especially for the structured region excluding the C-terminal tail (Figure 3b). The backbone ^{15}N T_2 relaxation times of Ala42 and Ser43 and those of the C-terminal tail, are far higher than the majority (Figure 3b), implying that these residues may be more conformationally mobile. The C-terminal tail is known to form part of the flexible linker that facilitates the movement of the lipoyl domain in reaching the three active sites of the complex (*1*). The surface loop linking β-strands 1 and 2 was poorly defined in the structure (Figure 1a) owing to the lack of long-range NOEs; the relaxation data imply that this region may have a degree of flexibility above that of the backbone. The other region poorly defined in the ensemble was the lipoyl-lysine β-turn region (Figure 1a). The relaxation parameters, especially for Ala42 and Ser43, were different from those of the general backbone, again indicating that this region is flexible.

Effect of Posttranslational Modification on the Structure of the E2plip Domain. The changes in $^1H^N$ and ^{15}N chemical shift that accompanied lipoylation of E2plip^{apo} are shown in Figure 4 (panels a and b). The largest changes occurred in

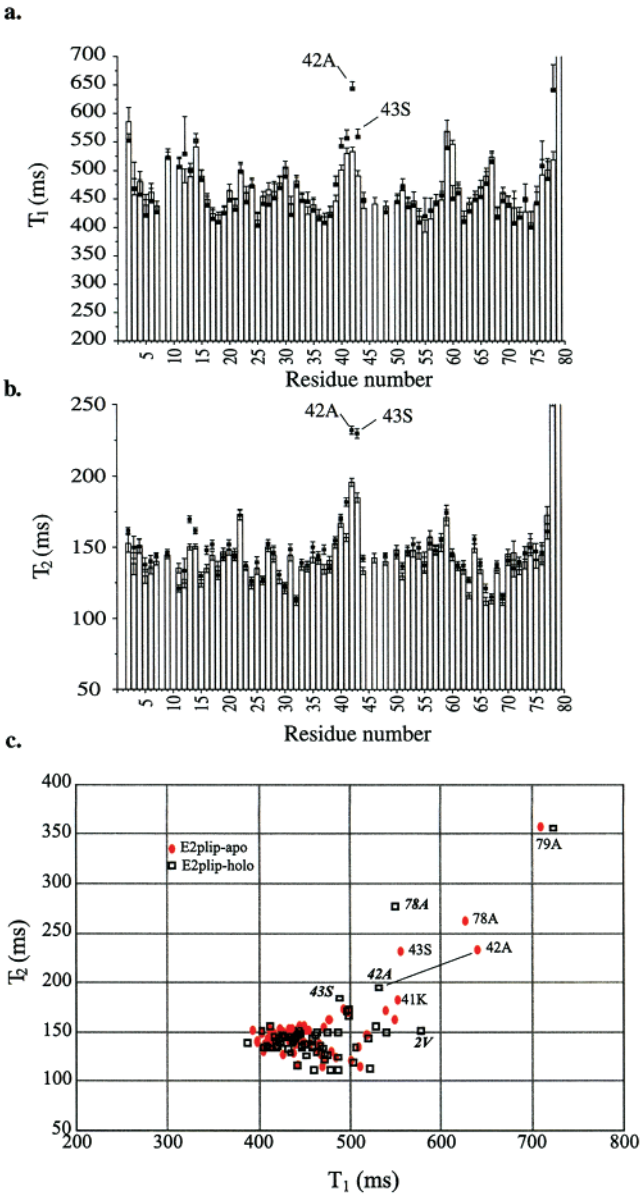

FIGURE 3: ^{15}N relaxation times of the apo- and holo-E2plip domains. E2plip^{apo} (■) and the E2plip^{holo} (shaded bars). (a) ^{15}N T_1 relaxation times of the E2plip^{apo} and E2lip^{holo} domains. (b) ^{15}N T_2 relaxation times of the E2plip^{apo} and E2lip^{holo} domains. (c) Plot of T_2 versus T_1. Key residues are identified in the diagrams. In panel c, residues indicated in italics are those of the holo-domain. Relaxation times were calculated from the resonance intensity from experiments with different delay times, as described in Materials and Methods. The error bars were calculated using the Monte Carlo method (*59*).

the region of the lipoyl-lysine β-turn, most notably residues Gly39, Glu40, Lys41, Ala42, Ser43, and Met44; the largest effective change in $^{1}H^{N}$ chemical shift was that for residue Lys41 (−0.298 ppm) and in the ^{15}N shift that for Ser43 (−2.488 ppm). Residues in the surface loop linking β-strands 1 and 2, plus residues in β-strand 2 and residues in and adjacent to β-strand 7 (even though the surface loop and β-strand 2 lie between it and the lipoyl-lysine), also underwent significant changes in chemical shift. However, these changes were much smaller than those in the lipoyl-lysine region. All the affected residues are close in space to the lipoyl-lysine side chain (Figure 1b).

Apart from residues in the lipoyl-lysine β-turn region, all the hetNOE values remained constant across the backbone on lipoylation of E2plip^{apo} (Figure 2b). Those of Gly39 and to a greater extent Asp40, Lys41, Ala42, and Ser43 became less negative and approached the backbone values after lipoylation of the domain, although the hetNOE values of Val2 and Asp13 remained below those of the main backbone, much as in the apo-domain. This suggests that the lipoyl-lysine β-turn region is becoming less flexible on lipoylation. The newly formed lipoyl-lysine side-chain amide [Lys-^{15}N-(H)-C(O)-lipoyl; 41Kζ] has a hetNOE value (−1.04) well below that of the backbone, suggesting that there is motion on the nanosecond to picosecond time scale about the lipoyl-lysine linkage, but this is still small compared with the flexible C-terminus, for which the hetNOE values were lower than −1.3 (Figure 2).

The relaxation properties of the E2plip^{holo} domain also differed from those of the E2plip^{apo} domain (Figure 3). Most of the ^{15}N T_1 relaxation times were not significantly affected, apart from two residues: Ala42 and Ser43 (Figure 3, panels a and c). The largest change in T_1 was for Ala42, where the relaxation time dropped from 644 ± 12 to 533 ± 8 ms on lipoylation of E2plip^{apo}, thus approaching the values for the majority of the backbone residues. The T_1 relaxation time of 41Kζ was 717 ± 9 ms, significantly higher than that of the majority of the backbone ^{15}N T_1 times.

The ^{15}N T_2 relaxation times for certain residues also exhibited significant changes on lipoylation of the domain. Residues Lys41 (lipoyl-lysine), Ala42, and Ser43 all underwent a large decrease in T_2, becoming closer to the general backbone T_2 times (Figure 3, panels b and c), with Ser43 undergoing the largest change (a decrease from 230 ± 3 ms to 185 ± 3 ms on lipoylation). The T_2 relaxation time of the 41Kζ amide was found to be 378 ± 6 ms, considerably higher than that observed for the majority of the ^{15}N nuclei of backbone residues. These decreases in both T_1 and T_2 relaxation times for certain residues close to the lipoyl-lysine suggest that this region of the protein is becoming less flexible on lipoylation.

As well as confirming that residues in the lipoyl-lysine β-turn, especially Ala42 and Ser43, have an associated decrease in mobility in the holo-domain compared with the apo-domain, Figure 3c also suggests there was a slight change in the overall tumbling. The correlation times (τ) calculated from the T_1/T_2 ratio (*39*) for residues considered to have no rapid internal motion were virtually identical within experimental error; τ for the E2plip^{holo} domain was 5.65 ± 0.54 ns, slightly higher than that for E2plip^{apo} (5.49 ± 0.51 ns). Moreover, the oscillation of both the apo- and holo-domain ^{15}N T_1 times confirms that the molecule is indeed ellipsoidal in shape.

Effect of Lipoylation on the H/D Exchange Rates of the E2plip Domain. For the most part, the H/D exchange rate of backbone amide protons thought to be involved in hydrogen bonds did not appear to undergo any change on lipoylation of the E2plip^{apo} domain. Quantitative analysis revealed that the backbone amide protons of four residues exchanged at a slower rate in the E2plip^{holo} domain: Val15, Glu16, Glu38, and Val46 (Figure 5). Val15 and Glu16 lie in β-strand 2 and Glu38 and Val46 in the β-strands 4 and 5, respectively, which form the lipoyl-lysine β-turn (Figure

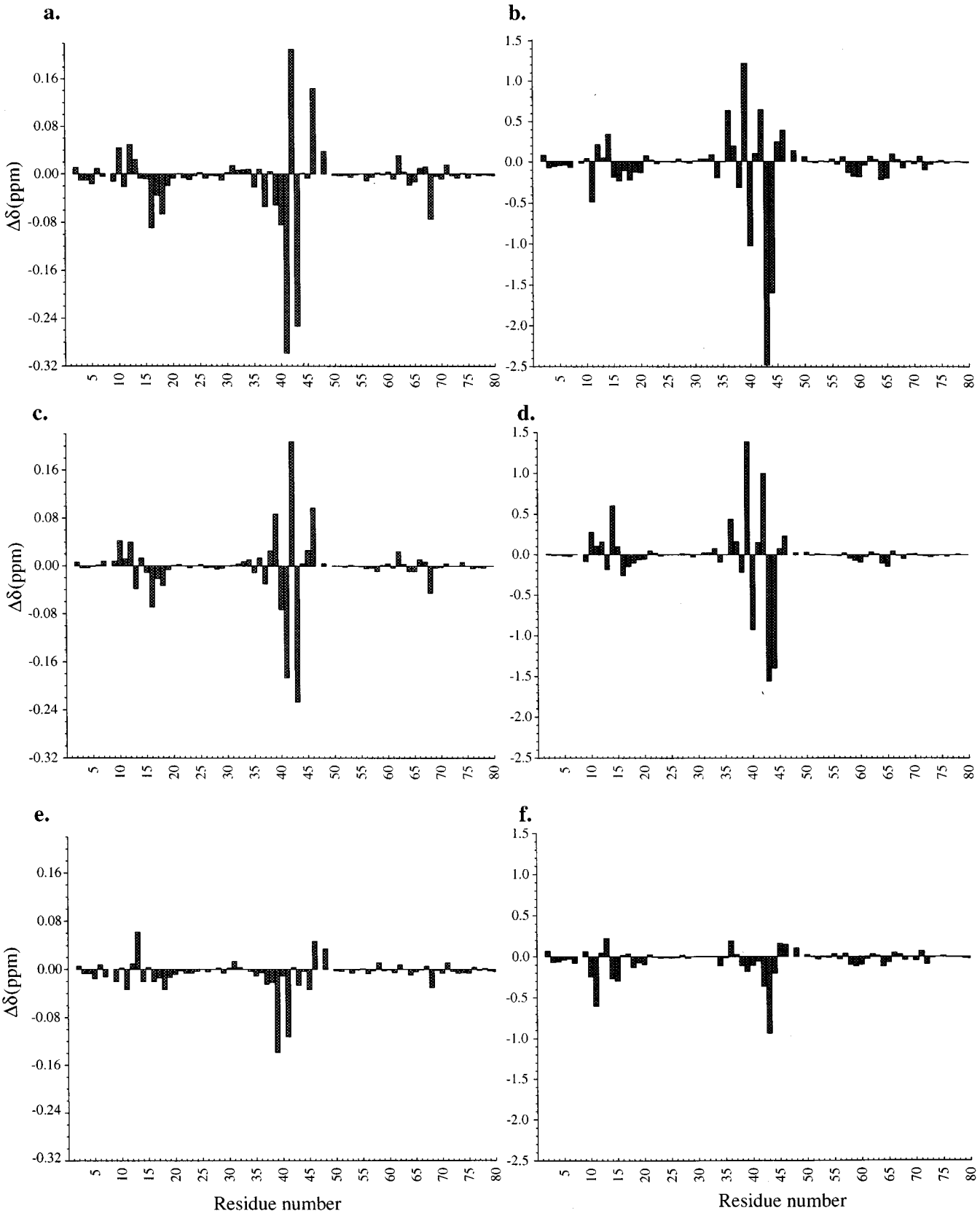

FIGURE 4: Chemical shift changes for the backbone H^N and N. Subtraction of the (a) H^N and (b) N $E2lip^{apo}$ chemical shifts from the $E2plip^{holo}$ chemical shifts; subtraction of the (c) H^N and (d) N $E2lip^{redac}$ chemical shifts from the $E2plip^{holo}$ chemical shifts; subtraction of the (e) H^N and (f) N $E2lip^{redac}$ chemical shifts from the $E2plip^{apo}$ chemical shifts.

1b). Nearby residues did not undergo any significant change in H/D exchange (Figure 5). The amide protons of Glu16 and Glu38 are part of a cross-strand hydrogen bond pair; the amide protons of Val15 and Glu46 are involved in a hydrogen bond with the carbonyl groups of Val65 and Ile35, respectively. The lipoyl-lysine side-chain amide proton was in fast exchange and is thus not involved in any hydrogen bond (data not shown).

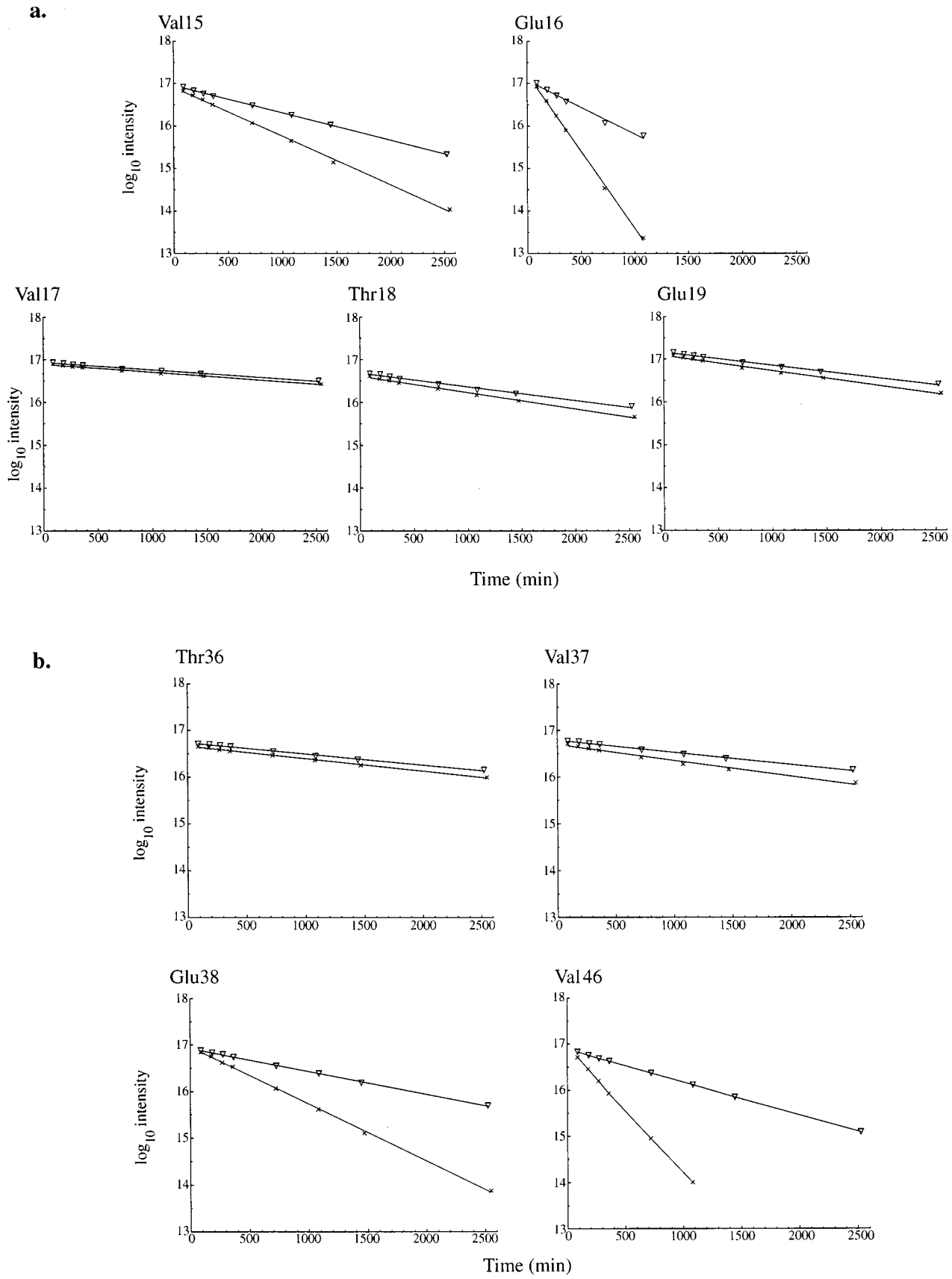

FIGURE 5: The H/D exchange rates of backbone amide protons for the E2plip^{apo} domain (×) and E2plip^{holo} domain (▽). H/D exchange rates for residues in (a) β-strand 2 (Val15, Glu16, Val18, and Glu19), (b) β-strand 4 (Thr36, Val37, and Glu38), and β-strand 5 (Val46). The rates were calculated by taking the log of the intensity of the cross-peaks from HSQC spectra recorded at various times after dissolving the lyophilized domain in ^2H_2O.

The decrease in H/D exchange rates of residues in secondary structure elements can be correlated with the decrease in flexibility within the lipoyl-lysine β-turn region indicated by the decreased relaxation times and the less

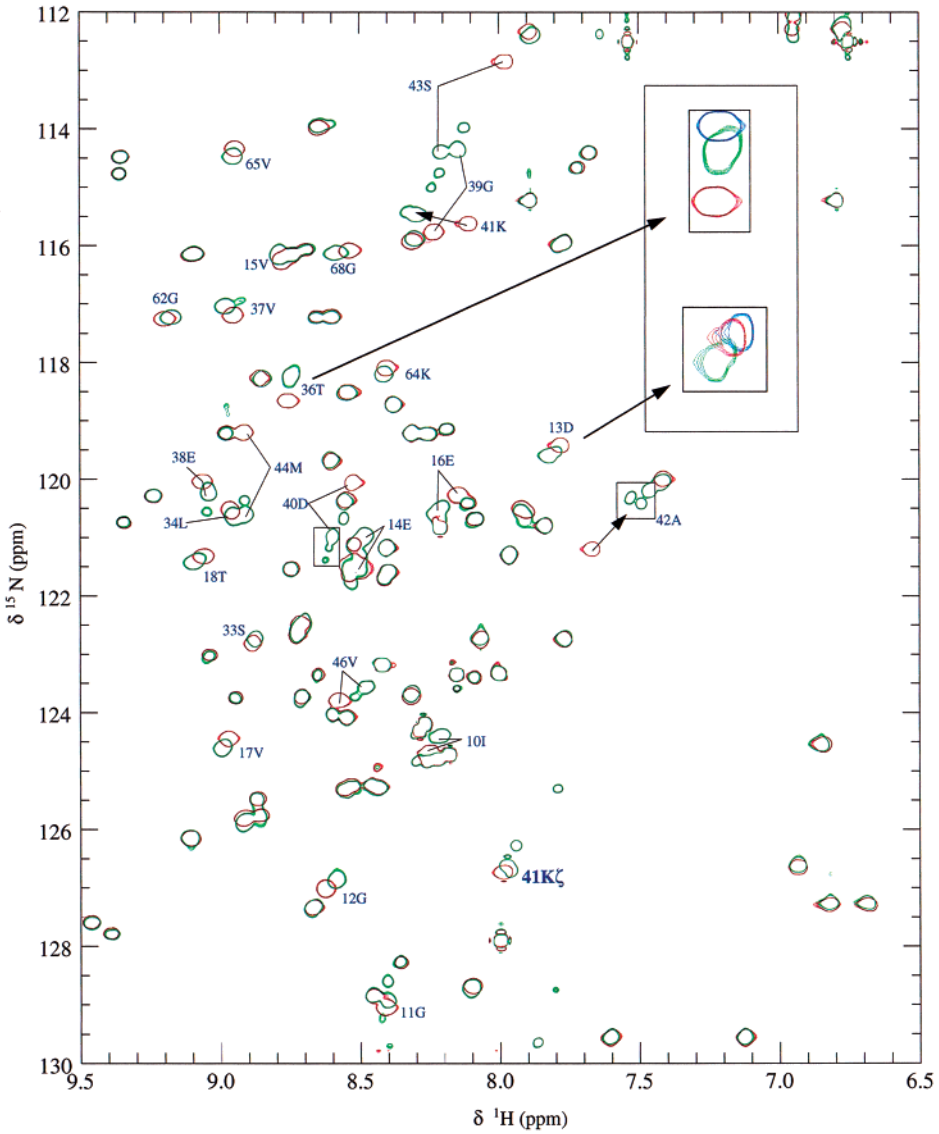

FIGURE 6: Comparison of the HSQC spectra of the E2plip^{holo} (red) and E2plip^{redac} (green) domains. Residues whose cross-peaks are considered to have undergone a significant change in chemical shift are indicated. E2plip^{redac} was generated from E2plip^{holo} as described in Materials and Methods. 41Kζ represents the side-chain lipoyl-lysine linkage [Lys-^{15}N(H)-C(O)-lip]. Cross-peaks associated with Asp13 and Thr36 have been magnified in the inset, with the blue cross-peaks representing those of the E2plip^{apo} domain. All spectra were recorded at 298 K and pH 6.85.

negative hetNOE values that accompanied lipoylation (Figures 2 and 3). If β-strands 4 and 5 become less flexible on lipoylation, hydrogen bonds in β-strands 4 and 5 and the adjacent β-strand 2 might be stronger than in the E2plip^{apo} form, consistent with a higher rate of H/D exchange. Another explanation might be that the lipoyl group is shielding the amide protons from the solvent, but this would require the lipoyl group to have a fixed orientation in the holo-domain.

Reductive Acetylation of the E2plip^{holo} Domain. Reductive acetylation of the E2plip^{holo} domain with a catalytic amount of E1p in the presence of pyruvate caused major changes to the HSQC spectrum (Figure 6). The attachment of the acetyl group to S^{8} and formation of the thiol group at S^{6} [HS-lip-S−C(O)-CH$_3$] (*55*) not only led to substantial changes in chemical shift but also to multiple resonances appearing for certain residues, most notably for residues in the lipoyl-lysine β-turn. At least three cross-peaks can be resolved for Asp40, Ala42, and Ser43, with many more residues showing double peaks (Figure 6). It was noted above that the acetyl-lipoyl thioester bond is unstable. An HSQC spectrum recorded approximately 24 h after the spectrum shown in Figure 6 showed extra cross-peaks not present in the initial HSQC spectrum (data not shown). It is likely that these extra resonances correspond to the deacetylated component.

Quantitative analysis of the changes in chemical shift accompanying reductive acetylation of the E2plip^{holo} domain revealed that the largest changes occurred in and around the lipoyl-lysine β-turn (Figure 4, panels c and d). The largest changes in the H^N and ^{15}N chemical shifts were associated with Ser43. Surprisingly, the change in chemical shift of the amide in the lipoyl-lysine side chain (41Kζ in Figure 6) was not as big as those for the backbone amides of the lipoyl-lysine β-turn region, even though it is the closest in terms of covalent structure to the reductively acetylated lipoyl group.

The chemical shifts for the E2plip^{apo} and E2plip^{redac} domains are more similar to each other than to the E2plip^{holo} spectrum. The changes in chemical shift of the residues in the lipoyl-lysine β-turn region are smaller between the E2plip^{apo} and E2plip^{redac} domains (Figure 4, panels e and f)

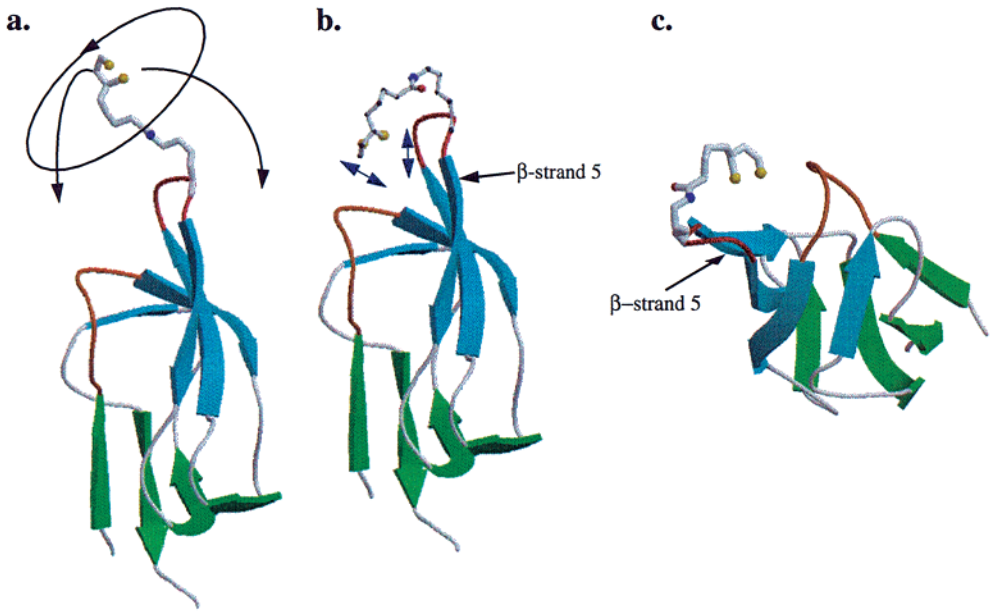

FIGURE 7: Speculative model for the positioning of the lipoyl group. (a) A freely rotating lipoyl group; (b and c) a lipoyl group with restricted mobility, close in space to the prominent surface loop. The lipoyl-lysine turn between β-strands 4 and 5 is shown in red, the surface loop between β-strands 1 and 2 in orange. The R-lipoate was attached to the domain using the program O (*60*) and structures were drawn using MOLSCRIPT (*58*).

than those observed when either domain is compared with the E2plip^{holo} domain (Figure 4, panels a−d). Moreover, the cross-peaks show a progressive movement from the E2plip^{holo} to the E2plip^{apo} spectrum via that of the E2plip^{redac} form (see Figure 6, Thr36 inset). The only exceptions to this are Gly39 and the residues in the surface loop linking β-strands 1 and 2. Some of the changes in chemical shift are larger and the progression between spectra observed for the other residues is not present (Figure 6, Asp13 inset).

DISCUSSION

It has generally been thought that the lipoyl group attached to the lipoyl domain of the E2p polypeptide is freely swinging as part of the lipoyl-lysine side chain. Such conclusions were based on spin-labeling experiments (*26*, *27*) and simple chemical shift analysis of NMR spectra (*28*, *29*). More detailed analysis of the spin-labeling experiments indicated that a fraction of the lipoyl groups had a different correlation time from the bulk, suggesting that these lipoyl groups might be immobilized (*56*). However, it was recognized that the derivatization of the lipoyl group with the nitroxide spin label might have induced differences from the native state.

More recently, the crystal structure of the pea leaf H-protein has indicated that the lipoyl group is localized by contact with a region of the protein equivalent to the surface loop linking β-strands 1 and 2 of the 2-oxo acid dehydrogenase lipoyl domains (*22*, *23*). NMR studies on the pea leaf H-protein have confirmed the original X-ray findings and revealed that the lipoyl-lysine β-turn and the contact region become less flexible upon lipoylation (*25*). The structure of the reductively aminomethylated (substrate-loaded) form of the H-protein showed that the chemically charged lipoyl group undergoes a large conformational change and becomes tucked into a nearby surface cleft on the protein, protecting the labile aminomethyl group (*23*, *25*).

The structure of the wild-type *E. coli* E2plip^{apo} domain closely resembles that of the previously determined hybrid domain (*14*), being composed of two four-stranded β-sheets with the lipoyl-lysine present at the tip of a type I β-turn (Figure 1b). The NMR relaxation studies reveal that two regions within the structure have greater flexibility than the majority of the backbone (Figures 2 and 3): the lipoyl-lysine β-turn and, to a lesser extent, the surface loop linking β-strands 1 and 2. The C-terminal tail, which forms part of the interdomain linker in the E2p chain, is also flexible, as expected.

Lipoylation of the E2plip^{apo} domain results in only minor changes to the overall structure of the domain, but the relaxation data suggest that the lipoyl-lysine β-turn becomes less flexible. This is supported by the stabilizing/shielding of several hydrogen bonds in β-strands 4 and 5, and the adjacent β-strand 2. The relaxation and hetNOE values for the side-chain lipoyl-lysine amide suggest that there is a degree of flexibility about that amide but not to the extent where it is freely swinging. Taken together, these results suggest interaction between the lipoyl group and the protein that restricts its motion, though not necessarily imposing complete immobilization.

From the chemical shift data, the most likely point of contact between the lipoyl group and the protein surface can be tentatively identified. When the domain was lipoylated, the largest changes in chemical shift occurred in the lipoyl-lysine β-turn region, more in β-strand 5 than β-strand 4 (Figure 4, panels a and b). The next largest effects were associated with the surface loop between β-strands 1 and 2 and the preceding β-strand 2, which lie close in space to the lipoyl-lysine. To a lesser extent, residues in and either side of β-strand 7 were also affected (Figure 4). Figure 7 shows a model for the location of the lipoyl-lysine side chain. Rather than being freely swinging (Figure 7a), the lipoyl group has a preferred orientation, pointing toward the surface loop linking β-strands 1 and 2 (Figure 7, panels b and c).

Restricting the movement of the lipoyl group would make good sense from the perspective of substrate channeling. For efficient reductive acetylation by the partner E1 to occur,

the lipoyl group must be attached to the lipoyl domain (*1*, *6*-*8*). Thus, E1 has to recognize the protein component transiently, as well as the prosthetic group. If the lipoyl group was freely swinging, the orientation of both the lipoyl group and the protein component would have to be momentarily correct in order to achieve catalysis. If the lipoyl group was in a preferred orientation, the approach of the protein component would enhance the likelihood of a productive encounter and an effective interaction with E1. On the basis of the recent crystal structure of the E1 ($\alpha_2\beta_2$) component of the branched chain 2-oxo acid dehydrogenase complex of *Pseudomonas putida*, it appears that the lipoyl group of the lipoyl domain must be fully protruding at the end of its lysine residue for it to reach the bottom of a 20 Å-long tunnel-shaped cavity, where the coenzyme, thiamin diphosphate, is located and where reductive acetylation takes place (*57*). The interaction with E1 is only transient, as the true substrate is the lipoylated domain. After reductive acylation, the lipoyl-lysine residue must withdraw, to permit the reductively acylated domain to visit the acyltransferase site in the inner core domain of E2 component, where the acyl group is transferred to CoA. There is no good evidence for a need to stabilize the thioester bond of the acyl-dihydrolipoyl group on the reductively acylated lipoyl domain, but structural changes to the lipoyl domain, notably in the surface loop between β-strands 1 and 2, can significantly diminish the stability of this thioester (*7*).

As well as the lipoyl-lysine β-turn region of the protein exhibiting large changes in chemical shift, residues in the surface loop are also affected on reductive acetylation. When comparing the HSQC spectra of the E2plip^{apo}, E2plip^{holo}, and E2plip^{redac} lipoyl domains, the chemical shifts of the E2plip^{apo} and E2plip^{redac} domains were closer to each other than to those of the E2plip^{holo} domain (Figure 4). The only exception to this was Gly39 and residues in the surface loop and preceding β-strand 2. All the other residues showed progressive changes from the E2plip^{holo} to E2plip^{redac} to E2plip^{apo} domains. This provides further evidence as to the positioning of the lipoyl group with respect to the protein and the potential role of the surface loop in stabilizing the acyl group attached to the dihydrolipoyl-lysine residue.

The changes in chemical shift between the E2plip^{holo} and E2plip^{redac} domains were larger than expected. In addition, the multiplicity of several resonances would suggest that multiple conformations are sampled by the E2plip^{redac} domain. There is no surface cavity present in the lipoyl domains of 2-oxo acid dehydrogenase complexes equivalent to that in the H-protein of the glycine cleavage system. However, the surface loop between β-strands 1 and 2 may play a similar role in stabilizing the reductively acylated group. Reductive acylation clearly results in important changes to the lipoyl domain in terms of structure or dynamics, and these warrant further investigation as to the part they may play in the catalytic mechanism.

ACKNOWLEDGMENT

We thank Dr. Pedro Reche for the gift of E1p, Dr. A. Raine for advice on X-PLOR, Dr. R.W. Broadhurst for help with the calculation of relaxation times, and Mr. C. Fuller for the preparation of LplA and skilled technical assistance.

SUPPORTING INFORMATION AVAILABLE

Chemical shift values for the innermost lipoyl domain of *E. coli* E2p. This information is available free of charge via the Internet at http://pubs.acs.org.

REFERENCES

1. Perham, R. N. (1991) *Biochemistry 30*, 8501−8512.
2. Berg, A., and de Kok, A. (1997) *Biol. Chem. 378*, 617−634.
3. de Kok, A., Hengeveld, A. F., Martin, A., and Westphal, A. H. (1998) *Biochim. Biophys. Acta 1385*, 353−366.
4. Reed, L. J., and Hackert, M. L. (1990) *J. Biol. Chem. 265*, 8971−8974.
5. Reed, L. J. (1974) *Acc. Chem. Res. 7*, 40−46.
6. Graham, L. D., Packman, L. C., and Perham, R. N., (1989) *Biochemistry 28*, 1574−1581.
7. Jones, D. D., Horne, H. J., Reche, P. A., and Perham, R. N. (2000) *J. Mol. Biol. 295*, 289−306.
8. Berg, A., Westphal, A. H., Bosma, H. J., and de Kok, A. (1998) *Eur. J. Biochem. 252*, 45−50.
9. Robien, M. A., Clore, G. M., Omichinski, J. G., Perham, R. N., Appella, E., Sakaguchi, K., and Gronenborn, A. M. (1992) *Biochemistry 31*, 3463−3471.
10. Kalia, Y. N., Brocklehurst, S. M., Hipps, D. S., Appella, E., Sakaguchi, K., and Perham, R. N. (1993) *J. Mol. Biol. 230*, 323−341.
11. Mande, S. S., Sarfaty, S., Allen, M. D., Perham, R. N., and Hol, W. G. J. (1996) *Structure 4*, 277−286.
12. Mattevi, A., Obmolova, G., Schulze, E., Kalk, K. H., Westphal, A. H., de Kok, A., and Hol, W. G. J. (1992) *Science 255*, 1544−1550.
13. Izard, T., Aevarsson, A., Allen, M. D., Westphal, A. H., Perham, R. N., de Kok, A., and Hol, W. G. J. (1999) *Proc. Natl. Acad. Sci. U.S.A. 96*, 1240−1245.
14. Green, J. D. F., Laue, E. D., Perham, R. N., Ali, S. T., and Guest, J. R. (1995) *J. Mol. Biol. 248*, 328−343.
15. Ricaud, P. M., Howard, M. J., Roberts, E. L., Broadhurst, R. W., and Perham, R. N. (1996) *J. Mol. Biol. 264*, 179−190.
16. Dardel, F., Davis, A. L., Laue, E. D., and Perham, R. N. (1993) *J. Mol. Biol. 229*, 1037−1048.
17. Berg, A., Vervoort, J., and de Kok, A. (1996) *J. Mol. Biol. 261*, 432−442.
18. Berg, A., Vervoort, J., and de Kok, A. (1997) *Eur. J. Biochem. 244*, 352−360.
19. Howard, M. J., Fuller, C., Broadhurst, R. W., Perham, R. N., Tang, J. G., Quinn, J., Diamond, A. G., and Yeaman, S. J. (1998) *Gastroenterology 115*, 139−146.
20. Wallis, N. G., and Perham, R. N. (1994) *J. Mol. Biol. 236*, 209−216.
21. Wallis, N. G., Allen, M. D., Broadhurst, R. W., Lessard, I. A. D., and Perham, R. N. (1996) *J. Mol. Biol. 263*, 436−474.
22. Pares, S., Cohen-Addad, C., Sieker, L., Neuburger, M., and Douce, R. (1994) *Proc. Natl. Acad. Sci. U.S.A. 91*, 4850−4853.
23. Cohen-Addad, C., Pares, S., Sieker, L., Neuburger, M., and Douce, R. (1995) *Nat. Struct. Biol. 2*, 63−68.
24. Macherel, D., Bourguignon, J., Forest, E., Faure, M., Cohen Addad, C., and Douce, R. (1996) *Eur. J. Biochem. 236*, 27−33.
25. Guilhaudis, L., Simorre, J. P., Blackledge, M., Neuburger, M., Bourguignon, J., Douce, R., Marion, D., and Gans, P. (1999) *Biochemistry 38*, 8334−8346.
26. Ambrose, M. C., and Perham, R. N. (1976) *Biochem. J. 155*, 429−432.
27. Grande, H. J., Van Telgen, H. J., and Veeger, C. (1976) *Eur. J. Biochem. 71*, 509−518.
28. Dardel, F., Laue, E. D., and Perham, R. N. (1991) *Eur. J. Biochem. 201*, 203−209.
29. Berg, A., de Kok, A., and Vervoort, J. (1994) *Eur. J. Biochem. 221*, 87−100.
30. Neidhart, F. C., Bloch, P. L., and Smith, D. F. (1974) *J. Bacteriol. 119*, 736−747.

31. Dardel, F., Packman, L. C., and Perham, R. N. (1990) *FEBS Lett. 264*, 206−210.
32. Reche, P., Li, Y. L., Fuller, C., Eichhorn, K., and Perham, R. N. (1998) *Biochem. J. 329*, 589−596.
33. Packman, L. C., Perham, R. N., and Roberts, G. C. K., (1984) *Biochem. J. 217*, 219−227.
34. Kraulis, P. J. (1989) *J. Magn. Reson. 84*, 627−633.
35. Piantini, U., Sorensen, O. W., and Ernst, R. R. (1982) *J. Am. Chem. Soc. 104*, 6800−6801.
36. Rance, M. (1987) *J. Magn. Reson. 74*, 557−564.
37. Kumar, A., Ernst, R. R., and Wüthrich, K. (1980) *Biochem. Biophys. Res. Commun. 95*, 1−6.
38. Norwood, T. J., Boyd, J., Heritage, J. E., Soffe, N., and Campbell, I. D. (1990) *J. Magn. Reson. 87*, 488−501.
39. Kay, L. E., Torchia, D. A., and Bax, A. (1989) *Biochemistry 28*, 8972−8979.
40. Barbato, G., Ikura, M., Kay, L. E., Pastor, R. W., and Bax, A. (1992) *Biochemistry 31*, 5269−5278.
41. Schirmer, R. E., Davis, J. P., Noggle, J. H., and Hart, P. A. (1972) *J. Am. Chem. Soc. 94*, 2561−72.
42. Farrow, N. A., Muhandiram, R., Singer, A. U., Pascal, S. M., Kay, C. M., Gish, G., Shoelson, S. E., Pawson, T., Forman Kay, J. D., and Kay, L. E. (1994) *Biochemistry 33*, 5984−6003.
43. Farrow, N. A., Zhang, O. W., Forman Kay, J. D., and Kay, L. E. (1995) *Biochemistry 34*, 868−878.
44. Pardi, A, Billeter, M, and Wüthrich, K. (1984) *J. Mol. Biol. 180*, 741−751.
45. Archer, S. J., Ikura, M., Torchia, D. A., and Bax, A. (1991) *J. Magn. Reson. 95*, 636−641.
46. Brünger, A. T. (1993) *XPLOR Manual, Version 3.1*, Yale University Press, New Haven, CT.
47. Nilges, M., Clore, G. M., and Gronenborn, A. M. (1988) *FEBS Lett. 239*, 129−136.
48. Collins, J. H., and Reed, L. J. (1977) *Proc. Natl. Acad. Sci. U.S.A. 74*, 4223−4227.
49. Laskowski, R. A., Macarthur, M. W., Moss, D. S., and Thornton, J. M. (1993) *J. Appl. Crystallogr. 26*, 283−291.
50. Brocklehurst, S. M., and Perham, R. N. (1993) *Protein Sci. 2*, 626−639.
51. Athappilly, F. K., and Hendrickson, W. A. (1995) *Structure 3*, 1407−1419.
52. Yao, X., Wei, D., Soden, C., Summers, M. F., and Beckett, D. (1997) *Biochemistry 36*, 15089−15100.
53. Roberts, E. L., Shu, N. C., Howard, M. J., Broadhurst, R. W., Chapman-Smith, A., Wallace, J. C., Morris, T., Cronan, J. E., and Perham, R. N. (1999) *Biochemistry 38*, 5045−5053.
54. Reddy, D. V., Rothemund, S., Shenoy, B. C., Carey, P. R., and Sönnichsen, F. D. (1998) *Protein Sci. 7*, 2156−2163.
55. Frey, P. A., Flournoy, D. S., Gruys, K., and Yang, Y. S. (1989) *Ann. N. Y. Acad. Sci. 573*, 21−35.
56. Ambrose Griffin, M. C., and Griffin, W. G. (1984) *Biochim. Biophys. Acta 789*, 87−97.
57. Ævarsson, A., Seger, K., Turley, S., Sokatch, J. R., and Hol, W. G. J. (1999) *Nat. Struct. Biol. 6*, 785−792.
58. Kraulis, P. J. (1991) *J. Appl. Crystallogr. 24*, 946−950.
59. Press, W. H., Flannery, B. P., Tuekolsky, S. A., and Vetterling, W. T. (1986) *Numerical Recipes*, Cambridge University Press, Cambridge.
60. Jones, T. A., Zou, J. Y., Cowan, S. W., and Kjeldgaard, M. (1991) *Acta Crystallogr., Sect. A 47*, 110−119.

BI992978I